PERKIN 2

Rotational barriers in tetraformylhydrazine

James A. Platts *[a] **and Michael P. Coogan** [b]

[a] *Dept. of Chemistry, Cardiff University, PO Box 912, Cardiff, UK CF10 3TB*
[b] *Dept. of Chemistry, Durham University, South Road, Durham, UK DH1 3LE*

Received (in Cambridge, UK) 22nd December 1999, Accepted 21st March 2000

Density functional calculations are reported on the various conformations of tetraformylhydrazine. These calculations indicate that rotation about the N–N bond is a relatively high-energy process, >140 kJ mol^{-1}, but that a multi-step pathway can yield the same result with substantially lower activation barriers of ≈80 kJ mol^{-1}. The calculated differences in barrier heights are rationalised on the basis of changes in geometrical and electron density properties. This analysis indicates the barrier to rotation about N–N in each case is dominated by destabilisation of N atoms and weakening of the N–N bond, but that the balance between steric and electronic factors determines the overall barrier. The calculations also suggest possible differences in spectroscopic properties that could be used to confirm the proposed low-energy pathway.

Introduction

Compounds which are chiral as a result of slow rotation around a bond are designated axially chiral or "atropisomeric".[1] The best known examples of this phenomenon are the biaryls, which have found great application in asymmetric synthesis, most importantly as ligands for metals in asymmetric catalysis,[2] however more recently the study of non-biaryl atropisomeric systems has also gained currency.[3] While the drive to develop new ligands for metals in asymmetric catalysis has led to the design of many analogues of the biaryl systems[4] little attention has been paid to the factors which lead to atropisomerism in the individual systems. As has recently been demonstrated by Tsue *et al.*,[5] a simplistic view of steric barriers to rotation (racemisation) can lead to fallacious assumptions. They demonstrated that in the simple heterobinaphthyl system the 8,8′-dialkyl-1,1′-biisoquinolines, increasing the steric bulk of the 8,8′ substituent *decreased* the barrier to racemisation.

One atropisomeric system which has attracted some interest recently is the N–N bond of peracyl hydrazines, or specifically *N*,*N*-diacyl-3-aminoquinazolinones which have been shown to be stable atropisomers.[6] Some years ago the barrier to rotation in tetraacyl hydrazines was measured by VT NMR and estimated to be variously 84–88[7] or 96–100 kJ mol^{-1},[8] and attributed to an unquantified combination of steric and polar or electronic effects. The exemplary tetraacyl hydrazines in these studies are cyclic imides, which could be regarded as possessing an intrinsically high steric barrier to rotation, unrepresentative of the parent tetraacyl hydrazine system. Recently a related system, the biquinazolinone, was shown by VT NMR to possess a minimum barrier to racemisation (rotation) of 85 kJ mol^{-1}, which could, however, be moderated by protonation, lending credence to a large electronic component to the barrier to rotation.[9] Here the ability to moderate the barrier to racemisation was utilised in a crystallisation induced deracemisation (asymmetric transformation) process. However, both for this approach to deracemisation to be more widely applied and for potential applications of the single enantiomers obtained to be viable, information regarding the barrier to racemisation and the factors which can affect it is required.

In order to obtain an estimate of the barrier to rotation about the N–N bond, and to investigate the electronic nature of this barrier, we have performed a detailed theoretical study of the simplest model compound, tetraformylhydrazine, $((HCO)_2N)_2$. Although not in itself chiral, a study of the rotation about the N–N bond in such a molecule can give an estimate of the intrinsic barrier to rotation of this bond, and allow us to deconvolute steric and electronic effects.

Computational methodology

All calculations were carried out using Gaussian98[10] running on EPSRC's Columbus facility. Several combinations of basis set and electron correlation treatments (HF, DFT, MP, CISD) (CISD = Configuration Interaction with Singles and Doubles) were checked for the small model system *N*-formylformamide, $HN(COH)_2$. From these calculations it was apparent that a proper description of geometries required at least a double-ξ basis set with polarisation and diffuse functions, and a density functional description of electron correlation. Subsequent calculations on $((HCO)_2N)_2$ were therefore performed using the B3LYP/6-31+G* methodology,[11,12] which has been shown[13] to yield barriers to rotation and inversion in good agreement with experiment. All stationary points on the potential energy surface were characterised as minima or transition states (TS's) by harmonic frequency calculations. Isotropic NMR data were calculated in Gaussian98 using the Gauge-Invariant Atomic Orbital (GIAO)[14] scheme. Calculation of NMR data, however, requires triple-ξ polarised basis sets,[15] so the GIAO procedure was repeated with the B3LYP/6-311++G** method at the B3LYP/6-31+G* optimised geometries. Identical calculations were carried out on tetramethylsilane (TMS) for comparison purposes.

Bonding and electronic properties were explored using the Atoms-in-Molecules (AIM) techniques pioneered by Bader and co-workers.[16] This is based around the definition of an interatomic surface, the 'zero-flux surface' in the gradient of the electron density of a molecule, and hence atomic basins, Ω. Atomic properties reported here are N, the electronic population, E, the atomic energy, V_{NE}, the overall electron–nuclear stabilisation energy, which includes inter- and intra-atomic effects, V_{NEO}, the atomic 'self-stabilisation' arising from the stabilisation of an atom's charge distribution by its own nucleus, and V_{REP}, the repulsive potential energy, composed of electron–electron and nucleus.

Bonding is another chemical concept which can be derived from the electron density, ρ, and its gradient. It has been shown[17] that two bonded atoms are joined by a single trajectory

DOI: 10.1039/a910230m

Table 1 Energies and geometrical parameters of stationary points

Conformation	Rel. energy/ kJ mol^{-1}	Point group	Imag. frequency	r(N–N)/Å	Sum of angles at N/°
I	0.0	D_{2d}	0	1.383	360.0
II	1.7	C_s	0	1.386	359.3
III	0.3	C_2	0	1.389	359.0
IV	142.0	D_2	1	1.413	360.0
V	131.8	C_1	1	1.442	359.6
VI	77.2	C_{2h}	1	1.437	360.0
VII	70.5	C_1	1	1.394	352.8[a]
VIII	60.1	C_1	1	1.397	351.7[a]

[a] For the N undergoing rotation about N–C.

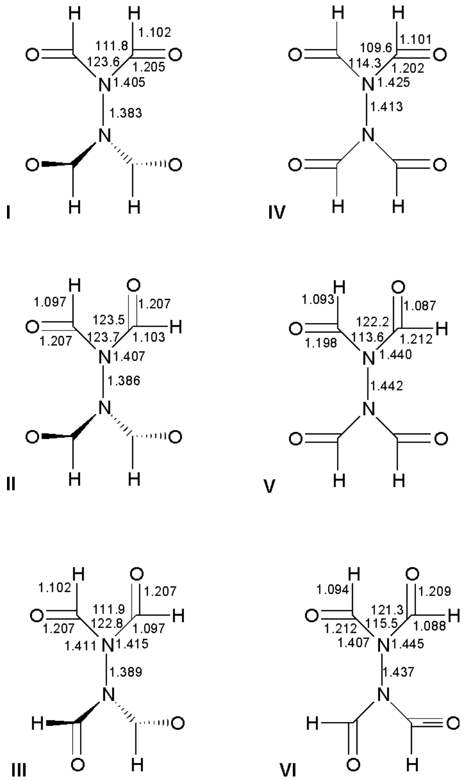

Fig. 1 Optimised geometries of conformations **I**–**VI**. Bond distances in Å, angles in °.

of the gradient of the electron density, termed the bond path. The point on the bond path where ρ reaches a minimum is denoted a bond or (3, −1) critical point (CP). Properties calculated at such points include ρ, the total electron density, which has been related to bond order,[18] $\nabla^2\rho$ the second derivative or Laplacian of the density, which measures the extent to which density is concentrated or depleted (more negative $\nabla^2\rho$ indicates greater concentration of charge). ε, the bond ellipticity, is often taken as a measure of π-bond character,[17] while the energy density per electron, E_d/ρ, has been proposed as a measure of bond energy.[19] Atomic and CP properties were calculated using the AIMPAC suite of programs,[20] in particular EXTREME and PROAIMV.

Results and discussion

Table 1 describes relative energies and some geometrical features of all the minima and transition states of tetraformylhydrazine found at the B3LYP/6-31+G* level, and Fig. 1 shows the optimised geometries of two minima and two TS's. In agreement with experiment,[21,22] the lowest energy conformation **I** is found to have D_{2d} symmetry, with each $(HCO)_2N$ fragment being exactly planar and the dihedral angle φ between these planes exactly 90°. The symmetrical arrangement of the $(HCO)_2N$ fragments also agrees with preliminary calculations on $(HCO)_2NH$, which is found to have C_{2v} symmetry only if electron correlation is accounted for by DFT, MP2 or CI methods.

Table 2 Optimised and crystal structure parameters of $((HCO)_2N)_2$. Distances in Å, angles in °

	B3LYP/6-31+G*	Experimental[a]
N–N	1.383	1.382
N–C	1.405	1.387
C=O	1.205	1.202
N–N–C	118.21	118.12
N–C–O	123.78	122.43
C–N–C	123.57	123.77
C–N–N–C	90.00	90.00

[a] Crystal structure from analysis taken from ref. 22.

Two crystal structures of $((HCO)_2)N)_2$ have been published,[21,22] both reporting the tetragonal space group I42m, in which each individual molecule has D_{2d} symmetry, exactly analogous to conformation **I**. Table 2 contains a comparison of our optimised structure with the more recent, and more accurate, crystal structure.[22] In general the agreement is excellent, with an average difference in heavy-atom bond lengths of 0.007 Å and angles of 0.55°. We can therefore take confidence that our calculations describe the important features of $((HCO)_2N)_2$.

Two other minima, **II** and **III**, with C_s and C_2 symmetry respectively, are found to be within 2 kJ mol^{-1} of the global minimum. These three minima differ in the relative geometry of the $(HCO)_2N$ fragments (see Fig. 1) and have φ either exactly or approximately 90°. That these conformations are so close in energy is confirmed by more accurate calculations on the C_{2v} and C_s conformations of $(HCO)_2NH$. These calculations also found a third conformer with each C=O bond parallel to the N–H bond, but this was of such high energy that it was discounted for the subsequent calculations on $((HCO)_2N)_2$.

Conformations **I**, **II**, and **III** can undergo rotation about the N–N bond, through TS's **IV**, **V**, and **VI**, respectively. Initial attempts to find **IV** assumed D_{2h} symmetry, with all atoms coplanar, but this resulted in a structure with two imaginary frequencies and very close O···O contacts. Relaxing the symmetry constraint to D_2 resulted in a TS structure with nitrogen atoms essentially planar and the C–N bonds eclipsed, but with the O and H atoms significantly out of this plane. This TS is over 140 kJ mol^{-1} higher in energy than **I**, a barrier so high that it is unlikely to be crossed under normal circumstances. Zero-point energy corrections reduce this barrier by less than 2 kJ mol^{-1}, while simulation of a DMSO solvation environment (using the SCRF-PCM model[23]) (SCRF-PCM = Self-consistent Reaction Field-Polarizable Continuum Model) lowered it by ≈6 kJ mol^{-1}. In the D_2 TS structure the O···O distances are 4.624 Å, almost 0.5 Å longer than in the D_{2d} structure: the presence of non-bonded O···O contacts is discussed in more detail below. **II** can rotate about N–N *via* **V** with a slightly reduced barrier of 130 kJ mol^{-1}, and here again a possible O···O contact is observed.

III, on the other hand, can rotate about N–N through TS **VI** with a barrier of just 77 kJ mol^{-1}, presumably as a result of the replacement of repulsive O···O contacts with O···H contacts. It is noteworthy that only TS **VI** is exactly planar, while both **IV** and **V** are distorted away from planarity. We suggest therefore that the barrier of 77 kJ mol^{-1} is due entirely to electronic effects, since no steric effects are present in **VI**. This electronic barrier is close to previous estimates[7–9] from VT NMR data of around 85 kJ mol^{-1}, albeit for rather different molecules.

N–N distances are similar for the three minima **I**, **II**, and **III** at approximately 1.386 Å, but lengthen substantially in the rotational TS's. This effect is smallest for the highest energy TS, **IV**, and much bigger in **V** and **VI**. We interpret this as evidence that the high energy of **IV** is due mainly to steric O···O contacts, rather than any extra weakening of the N–N bond. We also find that all three rotational TS's have essentially planar nitrogens, *i.e.* their angles sum to almost exactly 360°. Only in the TS's associated with rotation about N–C bonds **VII** and **VIII** are the nitrogens significantly non-planar, a fact well documented from studies of rotational barriers in amides.[24] Thus, rotation about N–N weakens and lengthens this bond, but does not significantly alter the planarity of each N.

Interconversion between **I**, **II**, and **III** is possible, and proceeds *via* two TS's, **VII** and **VIII**, which are approximately 70 and 60 kJ mol^{-1} higher in energy than **I**, respectively. Thus, there exists an alternative pathway (see Scheme 1) for rotation of **I** about the N–N axis, *i.e.* **I**→**II**→**III**→**III′**→**II′**→**I′** (where **I′** denotes **I** rotated about the N–N axis, and so on). No barrier on this pathway from **I** to **I′** is greater than 77 kJ mol^{-1}, such that **I** can effectively rotate to **I′** avoiding the 140 kJ mol^{-1} barrier noted above.

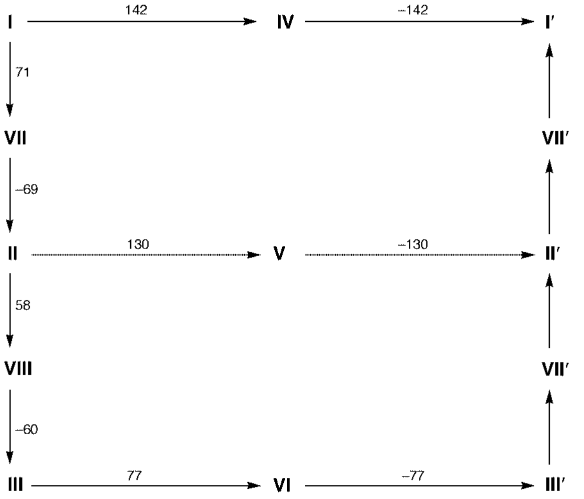

Scheme 1 Barriers to rotation (kJ mol^{-1}) about N–N and N–C bonds.

The two intermediates on this pathway, **II** and **III**, could conceivably be observed spectroscopically. VT NMR is the technique of choice in measuring barrier heights in systems such as these, and accordingly we report calculated ^{13}C chemical shifts relative to TMS for the three minima **I**, **II**, and **III** in Table 3. While the B3LYP/6-311++G**//B3LYP/6-31+G* method may give substantial absolute errors, it should suffice for comparisons between these minima. In **I**, all four C's are calculated to have δ 164.3, compared with an experimental figure of 172 ppm for C-substituted peracyl hydrazines.[25] Changing the orientation of one formyl group in **II** changes δ significantly; C4, the carbon in the rotated formyl group, is shifted downfield to 168.5 ppm. In **III** the difference is even more marked: C2 and C4 (those with C–H parallel to N–N) are more than 5 ppm downfield from C1 and C3. It may therefore prove possible to observe not only line broadening but also a shift to higher δ in ^{13}C VT NMR as rotation occurs.

Table 3 Calculated chemical shifts (ppm) for carbons in **I**, **II**, and **III**

Conformation	C1	C2	C3	C4
I	164.3	164.3	164.3	164.3
II	165.9	165.9	162.2	168.5
III	164.6	169.7	164.6	169.7

Table 4 N–N Bond critical point properties in **I**–**VII** (au)

Conformation	ρ	$\nabla^2\rho$	ε	$-E_d/\rho$
I	0.339	−0.635	0.000	0.943
II	0.337	−0.623	0.013	0.940
III	0.335	−0.614	0.019	0.937
IV	0.313	−0.534	0.158	0.892
V	0.294	−0.474	0.147	0.880
VI	0.299	−0.497	0.151	0.866
VII	0.329	−0.584	0.040	0.927
VIII	0.327	−0.577	0.024	0.925

Table 5 O···O and O···H Bond critical point properties in **IV**, **V** and **VI** (au)

Conformation		ρ	$\nabla^2\rho$
IV	O···O	0.019	+0.075
V	O···O	0.026	+0.077
V	O···H	0.032	+0.114
VI	O···H	0.031	+0.108

Table 4 contains electron density properties calculated at the N–N bond CP properties for **I**–**VIII**. The five conformations with $\varphi \approx 90.0$ show broadly similar properties in the N–N bond, while the remaining three (**IV**, **V**, and **VI**), which have $\varphi \approx 0.0$, show rather lower ρ and E_d/ρ, less negative $\nabla^2\rho$. This is characteristic of a decrease in covalency of the N–N bond, and suggests a substantial electronic contribution to the barrier heights in Table 1. There is, however, no correlation between changes in N–N bond length or CP properties and barrier height; **IV** is highest in energy of all eight conformations considered, but has rather less disruption of its N–N bond than either **V** or **VI**. This supports the assertion that the high barriers associated with **IV** and **V** have large steric contributions.

In the five conformations with $\varphi \approx 90.0$ bond CP's are found only between pairs of covalently bonded atoms. In those with $\varphi \approx 0.0$, however, CP's are found between atoms not formally bonded. **IV** has two bond and two ring CP's in the O···O close contact region, despite the distortion away from planarity of these atoms. In **V**, CP's are found in very similar positions, now with one O···O and one O···H interaction, while in **VI** two O···H interactions are present. The qualitative nature of these interactions can be inferred from electron density properties at the bond CP's, as shown in Table 5. All properties are characteristic of 'closed-shell' interactions such as hydrogen bonding,[17] but ρ in O···H CP's is up to 50% greater than in the O···O CP's. Thus the O···O contacts push electron density out of the internuclear region, and are associated with strongly repulsive steric interactions, while O···H contacts are much less repulsive, and may even be classified as weak C–H···O hydrogen bonds, a possibility discussed in more detail below.

Integrated atomic properties, most notably populations and energies, yield complementary information to the bonding arguments above. To simplify matters, we discuss only conformations **I**, **III**, **IV**, and **VI**, *i.e.* those involved in the highest and lowest N–N rotation barriers. Also, C, H, and O properties have been averaged for **III** and **IV** where these atoms are not

Table 6 Integrated atomic properties for **I**, **III**, **IV**, and **VI** (au)

Conformation		N	C	O	H
I	N	7.817	4.531	9.151	0.912
	E	−55.282	−37.118	−75.962	−0.585
	V_{NE}	−269.411	−152.844	−298.767	−13.715
	V_{NEO}	−133.806	−84.020	−185.108	−12.110
	V_{REP}	158.538	78.464	146.586	12.517
III	N	7.815	4.565	9.157	0.881
	E	−55.258	−37.138	−75.965	−0.574
	V_{NE}	−266.751	−153.071	−294.973	−13.741
	V_{NEO}	−133.758	−84.125	−185.134	−11.852
	V_{REP}	155.932	78.650	142.794	12.566
IV	N	7.786	4.565	9.127	0.915
	E	−55.177	−37.134	−75.981	−0.590
	V_{NE}	−264.442	−152.292	−298.332	−13.830
	V_{NEO}	−133.488	−84.140	−185.059	−12.167
	V_{REP}	153.777	78.506	146.115	12.621
VI	N	7.805	4.615	9.162	0.823
	E	−55.170	−37.178	−75.975	−0.561
	V_{NE}	−262.959	−153.703	−293.731	−13.246
	V_{NEO}	−133.511	−84.336	−185.201	−11.417
	V_{REP}	152.325	79.202	141.537	12.097

symmetrically equivalent; Table 6 contains these atomic properties. Considering first the high (140 kJ mol^{-1}) barrier from **I** to **IV**, we find substantial depopulation of both the N and O atoms accompanies rotation, but N is the only destabilised atom in the TS, each N being more than 275 kJ mol^{-1} less stable in **IV** than in **I**. The C and H atoms are stabilised and accept density, but each O is 50 kJ mol^{-1} more stable in the TS *despite* losing 0.024e in population. A more detailed analysis, decomposing the total energy changes into intra-atomic and inter-atomic stabilisation and repulsion, reveals that N is destabilised mainly through a loss of inter-atomic stabilisation, accompanied by smaller decreases in repulsion and intra-atomic stabilisation. C and H atoms are stabilised by an intra-atomic mechanism, presumably associated with their increase in population. O on the other hand stabilises itself by a large decrease in its overall repulsive energy, despite being involved in the O···O contacts discussed above. It seems that the loss of repulsion due to the shift of density to C outweighs any repulsive effects associated with the O···O contacts. This is an intriguing and we believe unprecedented interpretation of steric repulsive effects.

The pattern of atomic changes in the lower barrier, from **III** to **VI**, is somewhat different from above. Here the largest change in population is found in the H atoms, which lose almost 0.06 electron each. Both N's lose a smaller amount of density, but are very destabilised (231 kJ mol^{-1}); again this is the dominant energy change and the source of most of the barrier to rotation. As above, this is largely an inter-atomic effect, possibly as a result of the lengthening of the N–N bond, although the loss in population also leads to a smaller loss of self-stabilisation. C behaves in much the same fashion as in the higher barrier, but now each O gains a small amount of density, and is stabilised by around 13 kJ mol^{-1}. These changes support the idea that the O···H interactions are weak hydrogen bonds: Koch and Popelier[26] argue that increased population and stabilisation of O and decreased population and destabilisation of H are characteristics of all C–H···O hydrogen bonds. Thus, the barrier from **III** to **VI** has no steric contribution and the value of 77 kJ mol^{-1} may therefore be taken as an (admittedly rough) estimate of the electronic contribution to the other N–N rotation barriers.

The overall pattern of changes, both atomic and molecular, accompanying N–N rotation is broadly similar to those reported by Bader *et al.*[27] for rotation about the C–C bond of ethane. The TS is destabilised by a large loss of electron-nuclear attraction, not quite offset by a corresponding loss of repulsive energies, *i.e.* Case I in Bader's terminology. They also reported substantial weakening of the C–C bond in the TS, resulting from a shift of electron density away from the C–C bonding region, in much the same manner as we report above. Thus it seems the two rotations are similar in many ways, although the N–N rotation is complicated by the presence of O···O or O···H contacts in the transition state.

Conclusions

We calculate that direct rotation about the N–N bond of tetraformylhydrazine has a barrier of 140 kJ mol^{-1}, too high to be accessible under normal laboratory conditions. However, this barrier may be circumvented by successive rotation about two N–C amide bonds followed by rotation about N–N, a pathway which involves no barrier higher than 80 kJ mol^{-1}. Geometrical, topological and atoms-in-molecules analyses indicate that the higher barrier has approximately equal steric and electronic contributions, with the steric contacts evident in O···O 'bond' critical points. Conversely, weak C–H···O hydrogen bonds in the transition state suggest that the lower barrier to N–N rotation (77 kJ mol^{-1}) is almost exclusively electronic in origin.

Acknowledgements

We wish to thank the EPSRC for a generous grant of time on their Columbus facility.

References

1 E. L. Eliel, S. H. Wilen and L. N. Mander, *Stereochemistry of Organic Compounds*, Wiley, New York, 1994, ch. 14.5.
2 For reviews, see R. Noyori, *Asymmetric catalysis in Organic Synthesis*, Wiley & Sons, New York, 1994; K. Tomioka, *Synthesis*, 1990, 451.
3 J. Clayden, *Angew. Chem.*, *Int. Ed. Engl.*, 1997, **36**, 949.
4 See, for example G. Chelucci, A. Bacchi, D. Fabbri, A. Saba and F. Ulgheri, *Tetrahedron Lett.*, 1999, **14**, 553; X. Dai and S. Virgil, *Tetrahedron Asymmetry*, 1999, **10**, 25; T. Fukuda, R. Irie and T. Katsuki, *Synlett*, 1995, 197; R. W. Backer and M. V. Sargent, *Pure Appl. Chem.*, 1994, **66**, 2143.
5 H. Tsue, H. Fujinami, T. Itakura, R. Tsuchiya, K. Kobayashi, H. Takahashi and K. Hirao, *J. Chem. Soc.*, *Perkin Trans. 1*, 1999, 3677.
6 R. S. Atkinson, E. Barker, C. J. Price and D. R. Russell, *J. Chem. Soc.*, *Chem. Commun.*, 1994, 1159; G. A. El-Hiti, *Spectrosc. Lett.*, 1999, **32**, 671.
7 B. H. Korsch and N. V. Riggs, *Tetrahedron Lett.*, 1966, **47**, 5897.
8 S. M. Verma and R. Prasad, *J. Org. Chem.*, 1973, **38**, 1004.

9 M. P. Coogan, D. E. Hibbs and E. Smart, *Chem. Commun.*, 1999, 1991.

10 Gaussian98, Revision A.6, M. J. Frisch, G. W. Trucks, H. B. Schlegel, G. E. Scuseria, M. A. Robb, J. R. Cheeseman, V. G. Zakrzewski, J. A. Montgomery, Jr., R. E. Stratmann, J. C. Burant, S. Dapprich, J. M. Millam, A. D. Daniels, K. N. Kudin, M. C. Strain, O. Farkas, J. Tomasi, V. Barone, M. Cossi, R. Cammi, B. Mennucci, C. Pomelli, C. Adamo, S. Clifford, J. Ochterski, G. A. Petersson, P. Y. Ayala, Q. Cui, K. Morokuma, D. K. Malick, A. D. Rabuck, K. Raghavachari, J. B. Foresman, J. Cioslowski, J. V. Ortiz, B. B. Stefanov, G. Liu, A. Liashenko, P. Piskorz, I. Komaromi, R. Gomperts, R. L. Martin, D. J. Fox, T. Keith, M. A. Al-Laham, C. Y. Peng, A. Nanayakkara, C. Gonzalez, M. Challacombe, P. M. W. Gill, B. Johnson, W. Chen, M. W. Wong, J. L. Andres, C. Gonzalez, M. Head-Gordon, E. S. Replogle and J. A. Pople, Gaussian Inc., Pittsburgh, PA, 1998.

11 A. D. Becke, *J. Chem. Phys.*, 1993, **98**, 5648; C. Lee, W. Yang and R. G. Parr, *Phys. Rev. B*, 1988, **37**, 785.

12 R. Ditchfield, W. J. Hehre and J. A. Pople, *J. Chem. Phys.*, 1971, **54**, 724; M. S. Gordon, *Chem. Phys. Lett.*, 1980, **76**, 163.

13 G. R. DeMare and Y. Moussaoui, *Int. Rev. Phys. Chem.*, 1999, **18**, 91; X. F. Zhou, J. A. Krauser, D. R. Tate, A. S. van Buren, J. A. Clark, P. R. Moody and R. F. Liu, *J. Phys. Chem.*, 1996, **100**, 16822.

14 K. Wolinski, J. F. Hilton and P. Pulay, *J. Am. Chem. Soc.*, 1990, **112**, 8251.

15 P. R. Rablen, S. A. Pearlman and J. Finkbiner, *J. Phys. Chem. A*, 1999, **103**, 7357.

16 R. F. W. Bader, *Atoms in Molecule: A Quantum Theory*, Clarendon, Oxford, 1990.

17 R. F. W. Bader and H. Essen, *J. Chem. Phys.*, 1984, **80**, 1943.

18 R. J. Boyd and S. C. Choi, *Chem. Phys. Lett.*, 1985, **120**, 80; I. Alkorta, I. Rozas and J. Elguero, *Struct. Chem.*, 1999, **9**, 243.

19 S. Grimme, *J. Am. Chem. Soc.*, 1996, **118**, 1529; R. F. W. Bader, T. S. Lee, D. Cremer and E. Kraka, *J. Am. Chem. Soc.*, 1983, **105**, 5061.

20 F. W. Biegler-König, R. F. W. Bader and T.-H. Tang, *J. Comput. Chem.*, 1982, **3**, 317. These programs can be obtained from Prof. Bader, bader@mcmaster.ca, or from www.chemistry.mcmaster.ca/aimpac/

21 A. Hinderer and H. Hess, *Chem. Ber.*, 1974, **107**, 495.

22 T. Otterson, J. Almlof and J. Carle, *Acta Chem. Scand.*, *Ser. A*, 1982, **36**, 63.

23 S. Miertus, E. Scrocco and J. Tomasi, *Chem. Phys.*, 1981, **55**, 117.

24 K. B. Wiberg and K. E. Laidig, *J. Am. Chem. Soc.*, 1987, **109**, 5935.

25 M. P. Coogan, manuscript in preparation.

26 U. Koch and P. L. A. Popelier, *J. Phys. Chem.*, 1995, **99**, 9747.

27 R. F. W. Bader, J. R. Cheeseman, K. E. Laidig, K. B. Wiberg and C. Breneman, *J. Am. Chem. Soc.*, 1990, **112**, 6530.